Spatial variability of soil properties and its application in predicting surface map of hydraulic parameters in an agricultural farm

Priyabrata Santra*, U. K. Chopra and Debashis Chakraborty

Division of Agricultural Physics, Indian Agricultural Research Institute, New Delhi 110 012, India

Knowledge of spatial variation of soil properties is important in precision farming and environmental modelling. Spatial distribution of water content at field capacity (FC) and permanent wilting point (PWP) at different zones of a farm governs the available water for plant growth. These two soil hydraulic parameters play key roles in crop selection for different blocks of a farm, and in scheduling irrigation of crops in a field. In this study, spatial variation of bulk density organic carbon, silt and clay contents for two soil depths (0–15 and 15–30 cm) in the agricultural farm of the Indian Agricultural Research Institute, New Delhi were quantified and the respective surface maps were prepared through ordinary kriging. Particle size distribution shows better spatial correlation structure than bulk density and organic carbon content. Gaussian model fits well with experimental semivariogram of bulk density, and silt and clay contents. Hole-effect model was found to be the best to fit the experimental semivariogram of organic carbon content. Spatial correlation structure for both surface (0–15 cm) and subsurface (15–30 cm) soil layer remains the same, but the magnitude of spatial correlation differs. Cross-validation of the kriged map shows that spatial prediction of basic soil properties using semivariogram parameters is better than assuming mean of observed value for any unsampled location. Pedo-transfer functions were coupled with the surface map of basic soil properties to generate a map of water content at FC and PWP. Evaluation of spatial maps of θ_{FC} and θ_{PWP} showed reasonable accuracy of these two hydraulic parameters for farm-level or regional-scale application.

Keywords: Basic soil properties, ordinary kriging, pedo-transfer functions, semivariogram.

SOILS are characterized by high degree of spatial variability due to the combined effect of physical, chemical or biological processes that operate with different intensities and at different scales[1]. Knowledge of the spatial variation of soil properties is important in several disciplines, including agricultural field trial research and precision farming. Reports have shown that there is large variability in soil, crop, disease, weed and/or yield, not only in large-sized fields[2–5], but also in small-sized fields[6]. In precision farming, the concept of 'management zone' was evolved in response to this large variability with the main purpose in efficient utilization of agricultural inputs with respect to spatial variation of soils and its properties[7–9]. Moreover, use of simulation models in designing and testing of different land-use management options in agricultural farms increased substantially in the last few decades[10]. Therefore, an appropriate understanding of spatial variation of soil properties is essential for modelling at landscape scale. The most important way to gather knowledge in this aspect is to prepare soil maps through spatial interpolation of point-based measurements of soil properties.

Among different methods of spatial interpolation of soil properties, inverse distance weighing and ordinary kriging are most common[11,12]. From a theoretical standpoint, kriging is the optimal interpolation method[13]; however, its correct application requires an accurate determination of the spatial structure via semivariogram construction and model-fitting. At least 50 to 100 samples might be required to obtain a reliable semivariogram that correctly describes spatial structure[14]. Most of the studies showed the spatial variation of soil properties in plot or field scale (<100 ha area)[15–20] or in regular transect grids[21,22], but such information on farm or watershed scale with sparsely distributed irregular samples is meagre[23].

Estimating semivariogram parameters of soil properties using geostatistical tools and further applying them to predict other soil properties using ordinary kriging is the general procedure to prepare soil maps[1,13,21,24]. Till now, majority of the studies have dealt with variation of soil properties over two-dimensional surfaces. However, soil properties also vary largely along the depths due to active soil-forming processes of eluviation–illuviation down the soil horizon[25]. Characterization of soil below the surface is also important for proper management of water and nutrient in the root zone and in a broader perspective, for modelling of environmental processes[26]. In agricultural fields, modelling water flow and nutrient transport for efficient utilization of irrigation water and fertilizer needs information on surface as well as vertical variation of soil

*For correspondence. (e-mail: priyasan@rediffmail.com)

properties. Therefore, full characterization of soil in three-dimensional pedon needs the exploration of spatial structure behaviour of soil properties at different depths.

Water content at field capacity (FC) and permanent wilting point (PWP) are two most important hydraulic parameters which indicate plant-available soil water regime and help in scheduling irrigation to crops. Based on surface maps of these two hydraulic parameters, crops with specific water requirements may be selected for different locations in a farm. Direct measurement of these two parameters at multiple locations and preparation of surface map is difficult, time-consuming and costly. Moreover, as hydraulic properties are controlled by several landform processes, these are highly dynamic under field conditions. Alternately, these properties can be estimated from some basic soil properties using pedo-transfer functions (PTFs) in a non-spatial extent. Several region-specific PTFs have been developed throughout the world for estimating hydraulic properties from basic soil properties. These PTFs can, therefore, be used in generating maps of required hydraulic parameters.

In this article, we explore the possibility of fitting semivariogram models from irregularly sampled soil properties of an agricultural farm extending 243 ha in area. Secondly, difference in spatial variation of basic soil properties for two soil depths has been examined. Finally, spatial maps of basic soil properties for two soil depths were prepared using ordinary kriging and the respective maps of basic soil properties were used to generate maps of soil hydraulic parameters through linkage with suitable PTFs.

Materials and methods

Study area

This study was carried out at the experimental farm of the Indian Agricultural Research Institute (IARI), New Delhi (28°37′–28°39′N, 77°8′30″–77°10′30″E, 217–241 m amsl). The climate is semi-arid, June being the hottest and January the coldest months. Mean maximum temperature during summer months (May–July) varies between 43.9°C and 45°C. The temperature drops to a minimum of 5°C in January. Annual rainfall is 708.6 mm, of which 597 mm (84%) is received from June to September and the rest during winter months (November to March).

According to the soil survey report[27], there are six soil series in the IARI experimental farm under two broad soil subgroups – Typic Haplustepts and Typic Ustifluvent. These series are named as Mehrauli, Palam, Holambi, Daryapur, Nagar and Jagat. Sandy loam is the dominant soil textural class in the farm.

Soil sample collection and laboratory analysis

Soil samples were collected from 50 sites of the IARI farm (243 ha) covering six soil series under two soil subgroups (Figure 1). From each site, disturbed and undisturbed soil samples were collected from two depths: 0–15 and 15–30 cm. Core samplers with cylindrical cores of 7.1 cm diameter and 7.1 cm length were used for undisturbed soil sample collection, while disturbed soil samples were collected in polythene bags and air-dried in the laboratory. Disturbed samples were ground and passed through a 2 mm sieve, and used to determine soil texture[28], organic carbon and water content at FC (33 kPa) and PWP (1500 kPa)[29]. Undisturbed soil cores were oven-dried at 105°C and used to determine bulk density (ρ_b)[30].

Spatial variability of soil properties

Spatial variability is expressed by a semivariogram $\hat{\gamma}(h)$, which measures[1,24] the average dissimilarity between data separated by a vector h. It was computed as half the average squared difference between the components of data pairs:

$$\hat{\gamma}(h) = \frac{1}{2N(h)} \sum_{i=1}^{N(h)} [z(x_i) - z(x_i + h)]^2, \quad (1)$$

where $N(h)$ is the number of data pairs within a given class of distance and direction, $z(x_i)$ is the value of the variable at the location x_i and $z(x_i + h)$ is the value of the variable at a lag of h from the location x_i.

Experimental semivariogram value for each soil property was computed using GEOEAS (Geostatistical Environmental Assessment Software) and plotted with lag distance h. During pair calculation for computing the semivariogram, maximum lag distance was taken as half of the minimum extent of sampling area to minimize the border effect. Lag increment was fixed as 100 m. In this study, omnidirectional semivariogram was computed for each soil property because no significant directional trend was observed. The computed semivariogram values [$\hat{\gamma}(h)$] for corresponding lag (h) were fitted with available theoretical semivariogram models using weighed least square technique through solver function of MS Excel spreadsheet[31]. Weight for each lag was assigned according to the number of pairs for that particular lag. Best-fit model with lowest value of residual sum of squares was selected for each soil property and each soil depth. Three commonly used semivariogram models were fitted for each soil property. These are the spherical, exponential and Gaussian models. In the case of fitting the semivariogram for organic carbon content, hole-effect model was also included. Expressions for different semivariogram models used in this study are given below.

Spherical model:

$$\gamma(h) = C_0 + C\left[1.5\frac{h}{a} - 0.5\left(\frac{h}{a}\right)^3\right], \text{ if } 0 \le h \le a,$$
$$= C_0 + C, \text{ otherwise.} \quad (2)$$

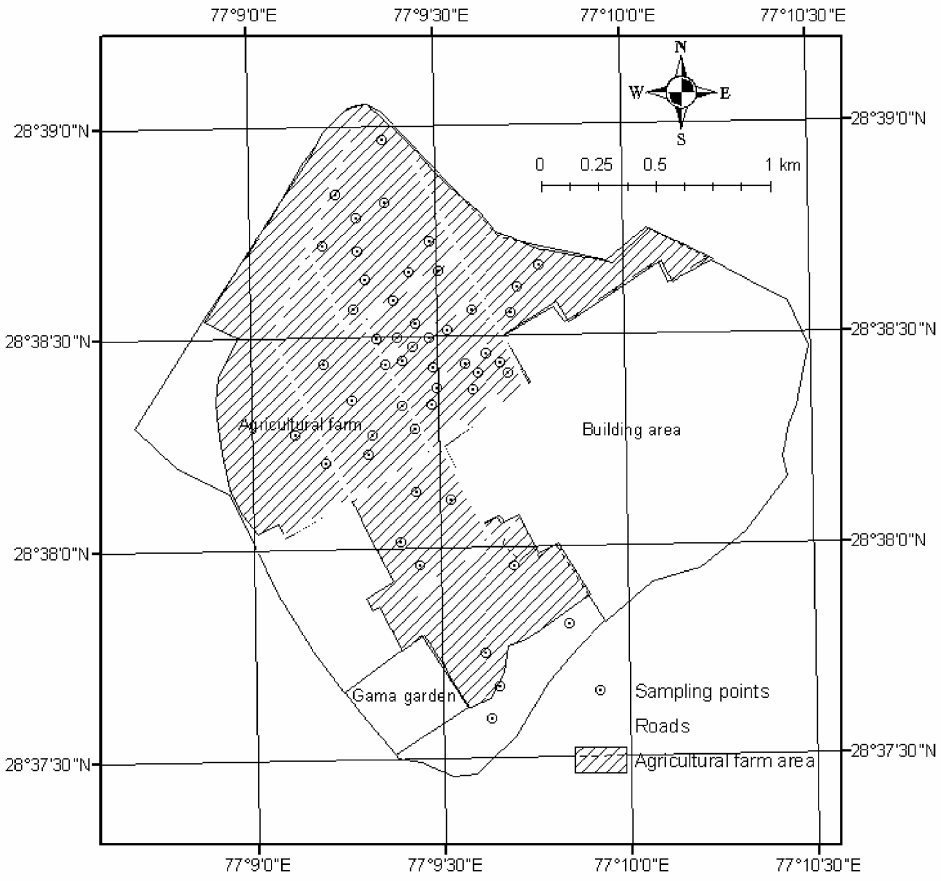

Figure 1. Location of sampling points in the experimental farm of the Indian Agricultural Research Institute, New Delhi.

Exponential model:

$$\gamma(h) = C_0 + C_1\left[1 - \exp\left\{-\frac{h}{a}\right\}\right] \quad \text{for } h \geq 0. \tag{3}$$

Gaussian model:

$$\gamma(h) = C_0 + C\left[1 - \exp\left\{\frac{-h^2}{a^2}\right\}\right] \quad \text{for } h \geq 0. \tag{4}$$

Hole-effect model:

$$\gamma(h) = C_0 + C_1\left[1 - \frac{\sin(\pi h/a)}{\pi h/a}\right] \quad \text{for } h \geq 0. \tag{5}$$

In all these semivariogram models, nugget, sill and range were expressed by C_0, $(C + C_0)$ and a respectively. In the case of exponential and Gaussian models, a represents the theoretical range. Practical range for these two semivariogram models was calculated as the lag distance for which the semivariogram value was 95% of sill.

Ordinary kriging of soil properties

Surface maps of basic soil properties were prepared using semivariogram parameters through ordinary kriging. Ordinary kriging estimates the value of soil attributes at unsampled locations, $z(u)$ using weighted linear combinations of known soil attributes $z(u_\alpha)$ located within a neighbourhood $W(u)$ centred around u.

$$z^*(u) = \sum_{\alpha=1}^{n(u)} \lambda_\alpha z(u_\alpha), \tag{6}$$

where λ_α is the weight assigned to datum $z(u_\alpha)$ located within a given neighbourhood $W(u)$ centred on u. The $n(u)$ weights are chosen so as to minimize the estimation or error variance $\sigma_E^2(u) = \mathrm{Var}\{z^*(u) - z(u)\}$ under the constraint of unbiasedness of the estimator. Kriged map for each soil property was prepared using geostatistical analysis tool of ArcGIS 9.1.

Accuracy of the soil maps was evaluated through cross-validation approach[32]. Among three evaluation indices used in this study, mean absolute error (MAE), and mean squared error (MSE) measure the accuracy of pre-

diction, whereas goodness-of-prediction (G) measures the effectiveness of prediction. MAE is a measure of the sum of the residuals (e.g. predicted minus observed)[22],

$$\text{MAE} = \frac{1}{N}\sum_{i=1}^{N}[|z(x_i) - \hat{z}(x_i)|], \tag{7}$$

where $\hat{z}(x_i)$ is the predicted value at location i. Small MAE values indicate few errors. The MAE measure, however, does not reveal the magnitude of error that might occur at any point and hence MSE will be calculated,

$$\text{MSE} = \frac{1}{N}\sum_{i=1}^{N}[z(x_i) - \hat{z}(x_i)]^2. \tag{8}$$

Squaring the difference at any point gives an indication of the magnitude, e.g. small MSE values indicate more accurate estimation, point-by-point. The G measure gives an indication of how effective a prediction might be, relative to that which could have been derived from using the sample mean alone[33],

$$G = \left(1 - \frac{\sum_{i=1}^{N}[z(x_i) - \hat{z}(x_i)]^2}{\sum_{i=1}^{N}[z(x_i) - \bar{z}]^2}\right) \times 100, \tag{9}$$

where $\bar{z}$ is the sample mean. If $G = 100$, it indicates perfect prediction, while negative values indicate that the predictions are less reliable than using sample mean as the predictors.

Preparation of surface map for water content at field capacity and permanent wilting point

Spatial maps on water content at field capacity (θ_{FC}) and permanent wilting point (θ_{PWP}) were prepared through linking soil maps on basic properties and PTFs. The PTFs for θ_{FC} and θ_{PWP} were developed from the available soil data in benchmark soils of India[34]. The performance of several existing PTFs was evaluated and compared with the developed PTFs using the measured water-retention data from the study area. It was found that the following PTFs developed from benchmark soils of India performed the best.

$$\theta_{FC}(\%, \text{w/w}) = 21.931 - 0.20564 \times \text{sand} + 0.175 \times \text{clay} + 4.6737 \times \text{OC} \quad (R^2 = 0.89), \tag{10}$$

$$\theta_{PWP}(\%, \text{w/w}) = 8.7255 - 0.092946 \times \text{sand} + 0.15944 \times \text{clay} \; (R^2 = 0.78), \tag{11}$$

where sand represents per cent sand content (0.05–2 mm), clay represents per cent clay content (< 0.002 mm) and OC is the per cent organic carbon content in the soils. These PTFs were used to convert the soil map of basic properties to hydraulic properties. Spatial prediction uncertainty of the developed map of θ_{FC} and θ_{PWP} was calculated by comparing them with their observed values at 50 locations of the study area.

Results and discussion

Descriptive statistics

Mean (μ) and standard deviation (σ) of soil properties are presented in Table 1. Before calculating the descriptive statistics, each soil property was checked for normality using the Kolmogorov–Smirnov (K–S) test statistics at 5% level of significance. Logarithmic transformations were made for silt content to fit it in normal distribution. Except silt content, other soil properties were fitted in normal distribution. Average bulk density for surface (0–15 cm) and subsurface (15–30 cm) layers was recorded as 1.54 and 1.62 Mg m^{-3} respectively. Intensive use of heavy tillage implements resulted in a compact layer at 15–30 cm soil depth. Organic carbon content at the surface was twice that of the subsurface, which might be due to continuous addition of crop residues on the surface of cropped fields. Among primary soil particles, silt content was slightly lower in the subsurface soil layer than the surface layer, whereas clay content was higher in the subsurface layer. Eluviation–illuviation process due to downward movement of water through the soil might have resulted in deposition of fine-size particles at greater depth. In general, the variation of bulk density and organic carbon content is higher in surface than subsurface soil layers, whereas the trend is reverse for silt content and clay content. Varieties of crops grown at different times and different blocks of the farm and the modified soil physical environment for each crop resulted in high variation of bulk density at the surface layer than subsurface layer. Moreover, differential growth behaviour of each crop results in different quantities of shoot and root biomass,

Table 1. Descriptive statistics of soil properties

Soil property	Depth (cm)	Mean	Standard deviation
Bulk density (Mg m^{-3})	0–15	1.54	0.09
	15–30	1.62	0.08
Organic carbon content (%)	0–15	0.62	0.22
	15–30	0.29	0.17
ln (% silt content)	0–15	2.51	0.27
	15–30	2.50	0.31
Clay content (%)	0–15	31.16	5.27
	15–30	33.42	6.59

Table 2. Residual sum of square for different theoretical semivariogram models used to fit the experimental semivariogram of soil properties at two depths

Soil property	Semivariogram model	Residual sum of square	
		0–15 cm depth	15–30 cm depth
Bulk density (Mg m^{-3})	Spherical	8.23×10^{-7}	10.6×10^{-7}
	Exponential	6.54×10^{-7}	9.33×10^{-7}
	Gaussian	**5.62×10^{-7}**	**8.05×10^{-7}**
Organic carbon content (%)	Spherical	4.89×10^{-5}	3.50×10^{-5}
	Exponential	5.85×10^{-5}	4.42×10^{-5}
	Gaussian	5.31×10^{-5}	4.42×10^{-5}
	Hole-effect	**4.23×10^{-5}**	**1.09×10^{-5}**
ln (% silt content)	Spherical	**4.82×10^{-5}**	39.90×10^{-5}
	Exponential	8.03×10^{-5}	39.30×10^{-5}
	Gaussian	11.30×10^{-5}	**36.80×10^{-5}**
Clay content (%)	Spherical	50.34	87.03
	Exponential	57.30	91.82
	Gaussian	**48.16**	**75.77**

Bold faced values are the lowest value of residual sum of square for a particular soil property and for a particular soil depth.

some of which were incorporated during tillage. For example, the amount of crop residue added over the soil surface is higher for cereal crops like rice, wheat and maize in comparison to pulse and oilseed crops. Hence, the variation of organic carbon content is higher in the surface layer than subsurface layer. Particle size distribution does not vary significantly in the surface soil layer. Mixing of soil during tillage operation resulted in less variation of particle size distribution at the surface layer than subsurface layer.

Semivariogram of soil properties

Residual sum of square for different theoretical semivariogram models (eqs (2)–(5)) to fit the experimental semivariogram values (Figure 2) for each soil property at two depths (0–15 and 15–30 cm) are given in Table 2. Among different theoretical models tested, the Gaussian model was found as the best fit in most cases. In case of organic carbon content, spatial variation for both the soil depths was best described by the hole-effect model. This indicates the periodic appearance of homogeneous patches of organic carbon content in two-dimensional spaces. The spherical model was best-fitted in only one case, i.e. for fitting the experimental semivariogram values for ln(silt) at 0–15 cm depth. Semivariogram parameters (range, nugget and partial sill) for each soil property with the best-fitted model are presented in Table 3. For bulk density and major textural separates, range varied from 900 to 1200 m. This indicate that bulk density, and silt and clay contents of two locations separated with lag distance below 1 km were spatially correlated with each other. Beyond this lag distance, the existing variation is defined as random variation. Organic carbon content was spatially correlated for a short lag distance, i.e. around 500 m. Nugget (C_0) defines the micro-scale variability and measurement error for the respective soil property, whereas partial sill (C) indicates the amount of variation which can be defined by spatial correlation structure. Out of the total variation, nugget component was 50% for bulk density, which shows that the micro-scale variation of this property was relatively high. Moreover, support area for measuring the bulk density was too small (7.1 cm in diameter) to average the micro-scale variations in the field. Minimum sampling distance in this study was 57.8 m, which may be too small to capture the variability at small lag. For organic carbon content, nugget component was around 75% of the total variance for 0–15 cm soil depth. For particle size distribution, nugget component was less than 50% for both silt and clay content. Silt content at 0–15 cm soil depth was found to be the best in terms of spatial correlation structure. Clay content was also highly spatially correlated and spatial correlation structure was better than that of bulk density and organic carbon content. Magnitude of spatial variance was higher in surface than subsurface layer for bulk density and organic carbon content, and reverse was the trend for silt and clay content. Similar findings were also pointed out from the classical statistical variance.

Kriging and cross-validation

Spatial maps prepared through ordinary kriging using the semivariogram parameters were cross-validated by leaving one sample out and predicting for that sample location based on rest of the samples. Evaluation indices resulting from cross-validation of spatial maps of soil properties are given in Table 4. Except for three cases the

Table 3. Semivariogram parameters of soil properties of IARI farm

Soil property	Depth (cm)	Semivariogram model	Range (m)	Nugget (C_0)	Partial sill (C)
Bulk density (Mg m^{-3})	0–15	Gaussian	1053	0.005	0.005
	15–30	Gaussian	1201	0.004	0.004
Organic carbon content (%)	0–15	Hole-effect	450	0.035	0.012
	15–30	Hole-effect	550	0.014	0.022
ln (% silt content)	0–15	Spherical	902	0.004	0.090
	15–30	Gaussian	1224	0.064	0.069
Clay content (%)	0–15	Gaussian	994	5.421	32.163
	15–30	Gaussian	1179	15.086	49.690

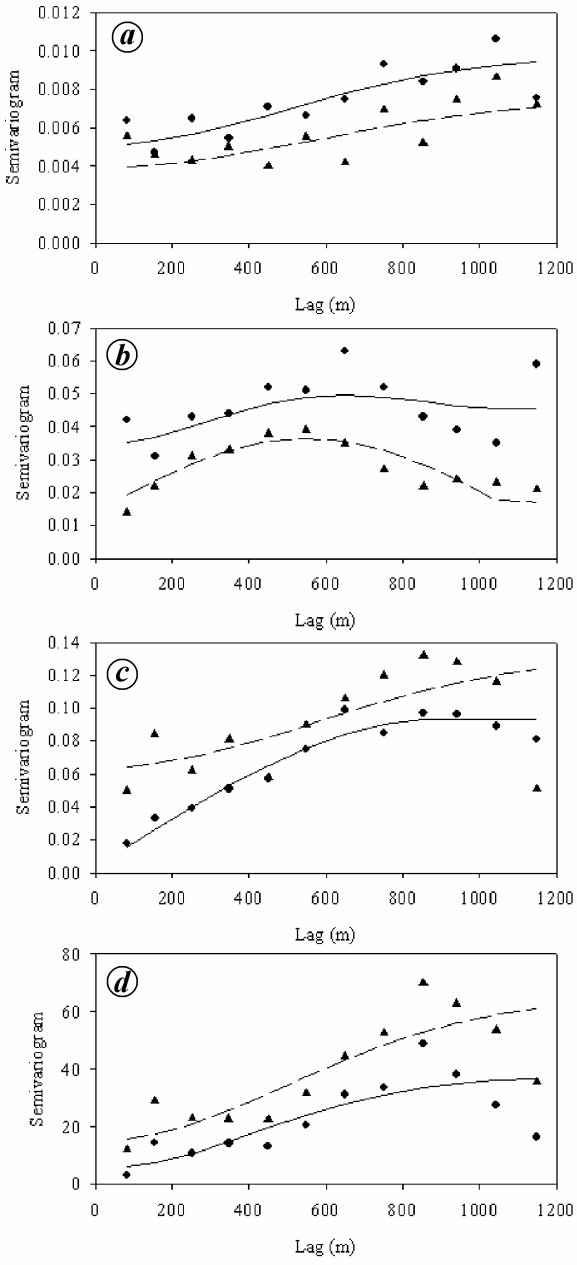

Figure 2. Semivariogram of soil properties. (***a***) Bulk density (Mg m^{-3}); (***b***) Organic carbon content (%); (***c***) ln (% silt content), and (***d***) Clay content (%).Experimental semivariogram for (•) 0–15 cm soil depth, (▲) 15–30 cm soil depth; Fitted semivariogram for (—) 0–15 cm soil depth, (----) for 15–30 cm soil depth.

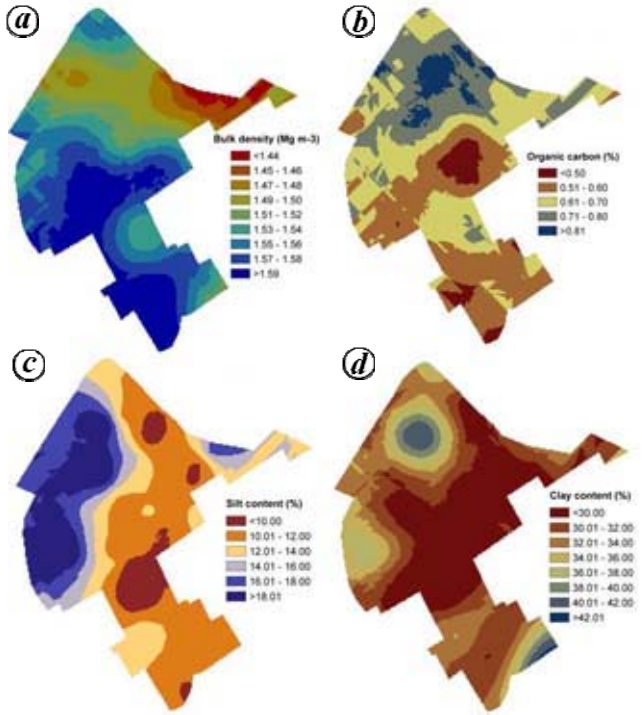

Figure 3. Krigged maps of soil properties for 0–15 cm soil depth. (***a***) Bulk density (Mg m^{-3}), (***b***) Organic carbon content (%), (***c***) Silt content (%), and (***d***) Clay content (%).

G value was greater than zero, which indicates that spatial prediction using semivariogram parameters is better than assuming mean of observed value as the property value for any unsampled location. This also shows that semivariogram parameters obtained from fitting of experimental semivariogram values were reasonable to describe the spatial variation. Although the *G* value for three cases was below zero, inclusion of more number of samples might have led to proper fitting of experimental semivariogram and describe the spatial variation in a better way.

Spatial maps of basic soil properties for 0–15 and 15–30 cm soil depth prepared through ordinary kriging are presented in Figures 3 and 4 respectively. The southern part of the farm is higher in bulk density (>1.59 Mg m^{-3}) at the surface, but lower at the subsurface than other parts of the farm (Figure 3 *a*). For the northwestern part of the farm, bulk density is 1.47–1.52 Mg m^{-3} at the surface and

Table 4. Evaluation performance of krigged map of soil physical properties through cross-validation

Soil property	Depth (cm)	MAE	MSE	G
Bulk density (Mg m^{-3})	0–15	0.074	0.008	–7.16
	15–30	0.053	0.005	18.90
Organic carbon content (%)	0–15	0.177	0.043	6.44
	15–30	0.132	0.032	–18.09
ln (% silt content)	0–15	0.175	0.051	29.21
	15–30	0.229	0.084	10.37
Clay content (%)	0–15	3.761	27.609	–1.51
	15–30	4.490	34.467	18.96

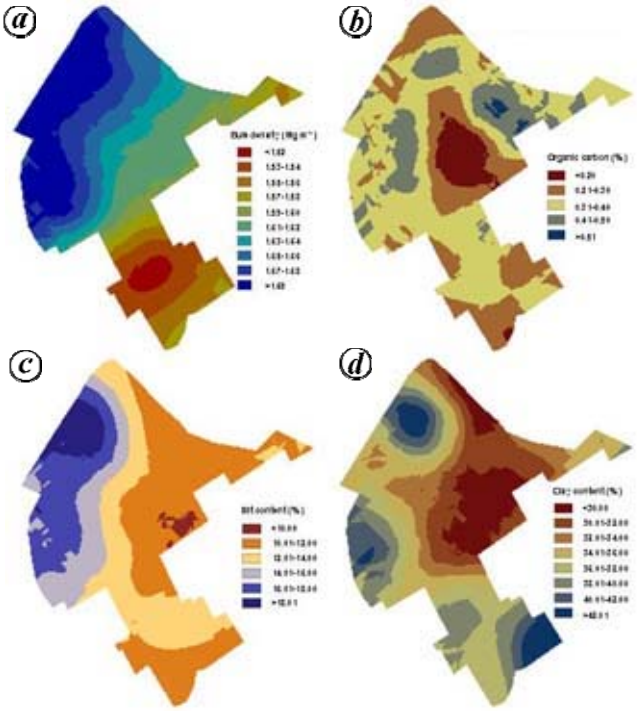

Figure 4. Krigged maps of soil properties for 15–30 cm soil depth. (***a***) Bulk density (Mg m^{-3}), (***b***) Organic carbon content (%), (***c***) Silt content (%), and (***d***) Clay content (%).

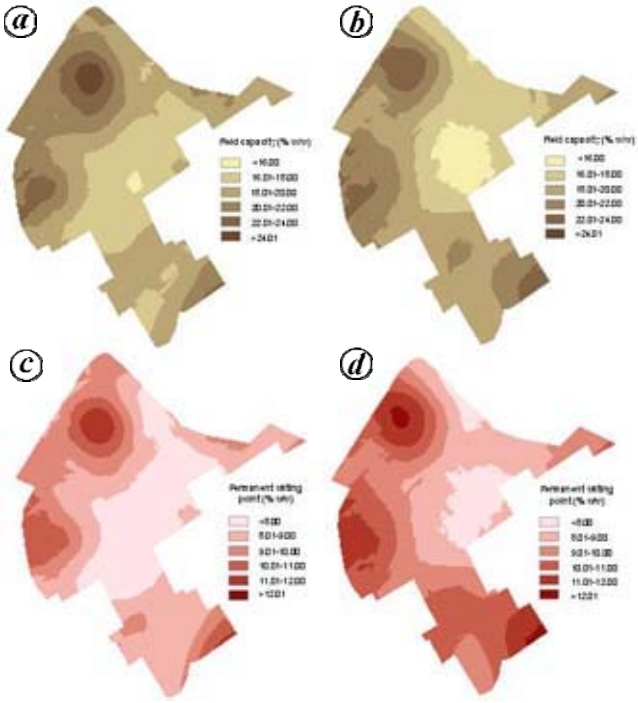

Figure 5. Spatially predicted map of water content for IARI farm. Water content at field capacity for 0–15 cm soil depth (***a***) and for 15–30 cm soil depth (***b***). Water content at permanent wilting point for 0–15 cm soil depth (***c***) and for 15–30 cm soil depth (***d***).

>1.67 Mg m^{-3} at the subsurface. This shows the presence of compacted subsurface layer in the northwestern part of the farm, possible due to continuous rice cultivation in these areas. Increase in bulk density in the east-to-west direction was also observed. Except for the southern part of the farm, a general trend of increase in bulk density with depth was observed. Spatial map of organic carbon content (0–15 cm) shows that 80% of the farm has medium organic carbon content (0.5–0.75%) and some patches of organic carbon content were also observed from the map (Figure 3 *b*). For the subsurface layer (Figure 4 *b*), the same pattern was followed with organic carbon content in low category (<0.5%) for maximum part of the farm. In general, organic carbon content was higher in the surface than subsurface layer for the entire farm area. Spatial map of silt content (%) shows that it decreases in the east-to-west direction for both surface (Figure 3 *c*) and subsurface (Figure 4 *c*) layers. The western part of the farm was slightly higher in silt content for the surface layer than subsurface layer. For other parts of the farm, there was no significant difference in silt content between the surface layer and subsurface layer. Figure 3 *d* shows that except a few patches, clay content was <34% for the surface layer. For subsurface layer (Figure 4 *d*), clay content was higher than the surface layer. For the western, northwestern and southwestern parts of the farm, clay content was around 4–6% higher in the surface than subsurface layer.

Spatial map of water content at field capacity and permanent wilting point

Spatial maps of θ_{FC} and θ_{PWP} were prepared by interpolating basic soil property followed by linking the maps using

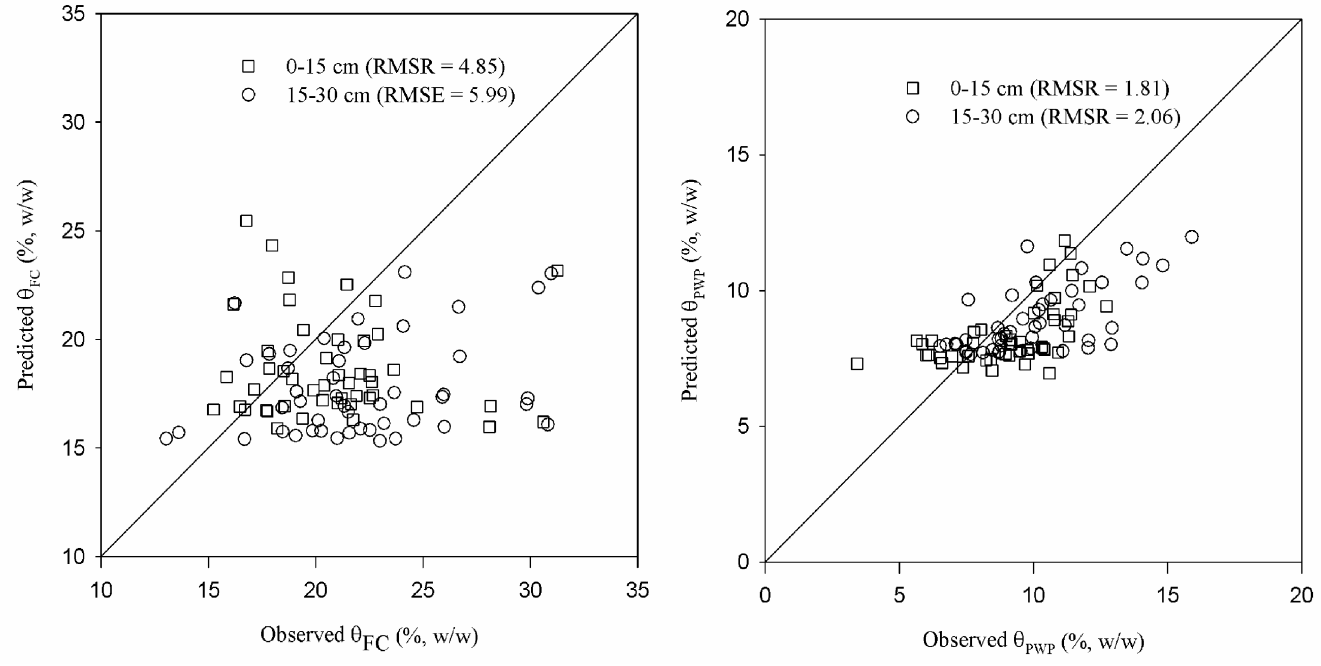

Figure 6. Observed values of water content at field capacity and permanent wilting point vs their predicted values from the respective spatial maps.

PTFs. Another way to generate the maps of θ_{FC} and θ_{PWP} is to predict the hydraulic parameters using PTFs and then by interpolating the point predicted values[35]. In the first approach, interpolation error for the map of basic soil property may be propagated multiple times, but the spatial maps of basic property may be further used for farm-level planning or modelling environmental processes. Moreover, in regionalized application, spatial map of hydraulic parameters generated through first approach will be significant[35]. Spatial maps of θ_{FC} and θ_{PWP} generated through the first approach are given in Figure 5. Water content at field capacity increased in the east-to-west direction of the farm for both surface and subsurface layers. The value of θ_{FC} (%, w/w) varied from 15.88 to 25.48% for the surface layer and 15.00 to 23.78% for the subsurface layer. Maximum water content was found at the northwestern part of the farm, where clay content was the highest. Similar type of spatial trend was also observed for the map of θ_{PWP}. The value of θ_{PWP} (%, w/w) varied from 6.72 to 11.92% for the surface layer and 7.52 to 12.21% for the subsurface layer. Spatial maps of θ_{FC} and θ_{PWP}, prepared from the map of basic soil properties and PTFs were evaluated on observed points of θ_{FC} and θ_{PWP}. Observed values of θ_{FC} and θ_{PWP} for the sampling locations in this study were plotted against their predicted values from the spatial maps (Figure 6). Scatter plot of observed and predicted values and their spread around the 1 : 1 line was better for θ_{PWP} than θ_{FC}. Root mean squared residual (RMSR) of predicted values of water content from the spatial map was 4.85–5.99% (w/w) and 1.81–2.06% (w/w) respectively, for θ_{FC} and θ_{PWP}. The magnitude of RMSR was almost same when these two hydraulic parameters were predicted from point measurements of basic soil property. Therefore, the spatial maps generated for θ_{FC} and θ_{PWP} may be used for farm-level planning of crop selection at different blocks of the farm. Spatial prediction uncertainty needs to be further tested for detailed application of such types of maps.

Conclusion

Bulk density and organic carbon content show large amount of nugget variation, which indicates the sum of micro-scale variation and error. Spatial correlation of bulk density and organic carbon content may be better described through sampling with fine grids. Particle size distribution shows better spatial correlation structure than bulk density and organic carbon content. Gaussian model fits the experimental semivariogram of basic soil properties better than other theoretical models, with exception for organic carbon content. Organic carbon content shows periodic variation over two-dimensional spaces. Therefore, the hole-effect model was found the best to fit the experimental semivariogram of organic carbon content. Spatial correlation structure for both surface and subsurface soil layers remains the same, but the magnitude of spatial correlation differs. For bulk density and organic carbon content, magnitude of spatial variance is higher in the surface than subsurface layer, whereas reverse is the trend for silt and clay content. Cross-validation of kriged map shows that spatial prediction of basic soil properties using semivariogram parameters is better than assuming mean of the observed value for any unsampled location.

Evaluation of spatial maps of θ_{FC} and θ_{PWP} showed reasonable accuracy of these two hydraulic parameters for farm-level or regional scale applications.

1. Goovaerts, P., Geostatistical tools for characterizing the spatial variability of microbiological and physico-chemical soil properties. *Biol. Fertil. Soil*, 1998, **27**, 315–334.
2. McBratney, A. B. and Pringle, M. J., Spatial variability in soil – Implications for precision agriculture. In Precision Agriculture 1997, Proceedings of the 1st European Conference on Precision Agriculture (ed. Stafford, J. V.), 1997, Oxford, UK, pp. 639–643.
3. Corwin, D. L. *et al.*, Assessment and field-scale mapping of soil quality properties of a saline–sodic soil. *Geoderma*, 2003, **114**, 231–259.
4. Godwin, R. J. and Miller, P. C. H., A review of the technologies for mapping within-field variability. *Biosyst. Eng.*, 2003, **84**, 393–407.
5. Vrindts, E., Mouazen, A. M., Reyniers, M., Martens, K., Maleki, M. R., Ramon, H. and De Baerdemaeker, J., Management zones based on correlation between coil compaction, yield and crop data. *Biosyst. Eng.*, 2005, **92**, 419–428.
6. Mouazen, A. M., Dumont, K., Maertens, K. and Ramon, H., Two dimensional prediction of spatial variation in topsoil compaction of a sandy loam field based on measured horizontal force of compaction sensor, cutting depth and moisture content. *Soil Till. Res.*, 2003, **74**, 91–102.
7. Franzluebbers, A. J. and Hons, F. M., Soil-profile distribution of primary and secondary plant-available nutrients under conventional and no tillage. *Soil Till. Res.*, 1996, **39**, 229–239.
8. Atherton, B. C., Morgan, M. T., Shearer, S. A., Stombaugh, T. S. and Ward, A. D., Site-specific farming: A perspective on information needs, benefits and limitations. *J. Soil Water Conserv.*, 1999, **54**, 455–461.
9. Malhi, S. S., Grant, C. A., Johnston, A. M. and Gill, K. S., Nitrogen fertilization management for no-till cereal production in the Canadian Great Plains: A review. *Soil Till. Res.*, 2001, **60**, 101–122.
10. Van Diepen, C. A., Van Keulen, H., Walf, J. and Berkhout, J. A. A., Land evaluation: From inhibition to quantification. *Adv. Soil Sci.*, 1991, **15**, 139–204.
11. Franzen, D. W. and Peck, T. R., Soil sampling for variable rate fertilization. In Proceeding of Illinois Fertilizer Conference (ed. Hoeft, R. G.), University of Illinois, Urbana-Champaign, IL, 1993, 25–27 January 1993, pp. 81–91.
12. Weisz, R., Fleischer, S. and Smilowitz, Z., Map generation in high-value horticultural integrated pest management: Appropriate interpolation methods for site-specific pest management of Colorado Potato Beetle (Coleoptera: Chrysomelidae). *J. Econ. Entomol.*, 1995, **88**, 1650–1657.
13. Isaaks, E. H. and Srivastava, R. M., *An Introduction to Applied Geostatistics*, Oxford Univ. Press, New York, 1989, p. 561.
14. Webster, R. and Oliver, M. A., Sample adequacy to estimate variograms of soil properties. *J. Soil Sci.*, 1992, **43**, 177–192.
15. Burgess, T. M. and Webster, R., Optimal interpolation and isarithmic mapping of soil properties: I. The semivariogram and punctual kriging. *J. Soil Sci.*, 1980, **31**, 315–331.
16. Diaz, O. A., Anderson, D. I. and Hanion, E. A., Soil nutrient variability and soil sampling in the everglades agricultural area. *Comm. Soil Sci. Plant Anal.*, 1992, **23**, 2313–2337.
17. Wollenhaupt, N. C., Wolkowski, R. P. and Clayton, M. K., Mapping soil test phosphorus and potassium for variable-rate fertilizer application. *J. Prod. Agric.*, 1994, **7**, 441–448.
18. Gotway, C. A., Ferguson, R. B., Hergert, G. W. and Peterson, T. A., Comparison of kriging and inverse-distance methods for mapping soil parameters. *Soil Sci. Am. J.*, 1996, **60**, 1237–1247.
19. Cassel, D. K., Wendroth, O. and Nielson, D. R., Assessing spatial variability in an agricultural experiment station field: Opportunities arising from spatial dependence. *Agron. J.*, 2000, **92**, 706–714.
20. Iqbal, J., Thomasson, J. A., Jenkins, J. N., Owen, P. R. and Whisler, F. D., Spatial variability analysis of soil physical properties of alluvial soils. *Soil Sci. Soc. Am. J.*, 2005, **69**, 1338–1350.
21. Trangmar, B. B., Spatial variability of soil properties in Sitiung, West Sumatra, Indonesia. Ph D dissertation, University of Hawaii, Honolulu, 1984.
22. Voltz, M. and Webster, R., A comparison of kriging, cubic splines and classification for predicting soil properties from sample information. *J. Soil Sci.*, 1990, **41**, 473–490.
23. Schloeder, C. A., Zimmermen, N. E. and Jacobs, M. J., Comparison of methods for interpolating soil properties using limited data. *Soil Sci. Soc. Am. J.*, 2001, **65**, 470–479.
24. Warrick, A. W., Myers, D. E. and Nielsen, D. R., Geostatistical methods applied to soil science. In *Methods of Soil Analysis, Part 1. Physical and Mineralogical Methods* (eds Klute, A. *et al.*), Agronomy Monograph No. 9, ASA, Madison, WI, 1986, 2nd edn, pp. 53–82.
25. Wilding, L. P., Spatial variability: Its documentation, accommodation and implication to soil surveys. In *Soil Spatial Variability* (eds Nielsen, D. R. and Bouma, J.), Pudoc, Wageningen, 1984, pp. 166–193.
26. Park, S. J. and Vlek, P. L. G., Environmental correlation of three-dimensional soil spatial variability: A comparison of three adaptive techniques, *Geoderma*, 2002, **109**, 117–140.
27. NBSS&LUP, Soil survey and land use planning of the IARI farm. National Bureau of Soil Survey and Land Use Planning, New Delhi, 1976.
28. Bouyoucos, G. J., Hydrometer method improved for making particle size analysis of soils. *Agron. J.*, 1962, **54**, 464–465.
29. Klute, A. and Dirkson, C., Hydraulic conductivity and diffusivity: Laboratory methods. In *Methods of Soil Analysis. Part 1. Physical and Mineralogical Methods* (ed. Klute, A. *et al.*), Agronomy Monograph No. 9, ASA, Madison, WI, 1986, 2nd edn, pp. 687–734.
30. Blake, G. R. and Hartge, K. H., Bulk density. In *Methods of Soil Analysis, Part 1. Physical and Mineralogical Methods* (eds Klute, A. *et al.*), Agronomy Monograph No. 9, ASA, Madison, WI, 1986, 2nd edn, pp. 363–375.
31. Jian, X., Olea, R. A. and Yu, Y., Semivariogram modeling by weighted least squares. *Comp. Geosci.*, 1996, **22**, 387–397.
32. Davis, B. M., Uses and abuses of cross-validation in geostatistics. *Math. Geol.*, 1987, **19**, 241–248.
33. Agterberg, F. P., Trend surface analysis. In *Spatial Statistics and Models* (eds Gaile, G. L. and Willmott, C. J.), Reidel, Dordrecht, The Netherlands, 1984, pp. 147–171.
34. Murthy, R. S., Hirekerur, L. R., Deshpande, S. B., Venkata Rao, B. V. and Shankaranarayana, H. S., *Benchmark Soils of India – Morphology, Characteristics and Classification for Resource Management*, NBSS&LUP, Nagpur, 1982, p. 373.
35. Bechini, L., Bocchi, S. and Maggiore, T., Spatial interpolation of soil physical properties for irrigation planning. A simulation study in northern Italy. *Eur. J. Agron.*, 2003, **19**, 1–14.

ACKNOWLEDGEMENTS. The first author acknowledges the help rendered by Prof. B. S. Das, IIT Kharagpur during the development of PTFs from benchmark soils of India. Financial support in the form of Junior Research Fellowship to the first author provided by ICAR, New Delhi during this study is acknowledged.

Received 25 April 2008; accepted 1 August 2008